Coupling of the $X\ ^1\Sigma^+$ and $a\ ^3\Sigma^+$ states of KRb

A. Pashov
Department of Physics, Sofia University, 5 James Bourchier Boulevard, 1164 Sofia, Bulgaria

O. Docenko, M. Tamanis, and R. Ferber
Department of Physics and Institute of Atomic Physics and Spectroscopy, University of Latvia, 19 Rainis Boulevard, Riga LV-1586, Latvia

H. Knöckel and E. Tiemann
Institut für Quantenoptik, Leibniz Universität Hannover, Welfengarten 1, 30167 Hannover, Germany
(Received 19 June 2007; published 30 August 2007)

A comprehensive study of the electronic states at the $4s+5s$ asymptote in KRb is presented. Abundant spectroscopic data on the $a\ ^3\Sigma^+$ state were collected by Fourier-transform spectroscopy, which allows one to determine an accurate experimental potential energy curve up to 14.8 Å. The existing data set [C. Amiot *et al.*, J. Chem. Phys. **112**, 7068 (2000)] on the ground state $X\ ^1\Sigma^+$ was extended by several additional levels lying close to the atomic asymptote. In a coupled channels fitting routine complete molecular potentials for both electronic states were fitted. Along with the line frequencies of the molecular transitions, recently published positions of Feshbach resonances in ^{40}K and ^{87}Rb mixtures [F. Ferlaino *et al.*, Phys. Rev. A **74**, 039903 (2006)] were included in the fit. This makes the derived potential curves capable for an accurate description of observed cold collision features so far. Predictions of scattering lengths and Feshbach resonances in other isotopic combinations are reported.

DOI: 10.1103/PhysRevA.76.022511 PACS number(s): 31.50.Bc, 33.20.Kf, 33.20.Vq, 33.50.Dq

I. INTRODUCTION

Along with NaK and NaRb, the KRb molecule is one of the most extensively studied among the mixed alkali-metal dimers. The ground state $X\ ^1\Sigma^+$, the lowest singlet states, and some of the triplet states were studied by various spectroscopic techniques. It is therefore surprising that the triplet state $a\ ^3\Sigma^+$ was not characterized experimentally so far.

In recent years, understanding interactions between different alkali-metal species in their singlet and triplet ground states of the pairs became important due to the experiments in mixed atomic traps. This stimulated investigations of the molecular states as well. Using molecular spectroscopy, several ground state asymptotes were examined: NaRb [1], NaCs [2], LiCs [3]. In the present study we applied the same technique for KRb. This molecule is particularly interesting since several groups are operating two-species traps, cold KRb molecules have been already formed, positions of several Feshbach resonances in ^{40}K^{87}Rb have been measured [4–6], and new ones are still being searched for. The study of the $(4s)$K+$(5s)$Rb asymptote has therefore several strong motivations: (i) to obtain complete and accurate potentials for the $X\ ^1\Sigma^+$ and $a\ ^3\Sigma^+$ states, to be able to model cold collisions; (ii) to prove the validity of the isotopic scaling rules, i.e., applying the potentials derived for the main isotopic combination ^{39}K^{85}Rb to reproduce the experimental observations (including the Feshbach resonances) in other isotopes of KRb; and (iii) to predict new Feshbach resonances that can be later verified and precisely measured experimentally with much reduced effort for the search procedure.

Along with the theoretical calculations of the long range dispersion coefficients [7–10] there are two theoretical works devoted to the study of the electronic structure of KRb [11,12] and one [13] where dipole moments were calculated. Figure 1 shows selected electronic states from Ref. [11] and should be helpful later in understanding the excitation steps in the experiment.

The ground state $X\ ^1\Sigma^+$ of KRb was first studied for $v''\leq 44$ at high resolution by Ross and co-workers [14]. A significant step toward the asymptote was done in Ref. [15], where an accurate potential energy curve for v'' up to 87 was derived. In both investigations the laser-induced fluorescence to the KRb ground state was recorded by exciting the $A\ ^1\Sigma^+$ state by radiation of a Ti:sapphire laser. The $B(1)\ ^1\Pi$ state was studied in Refs. [16–18]. Numerous perturbations were

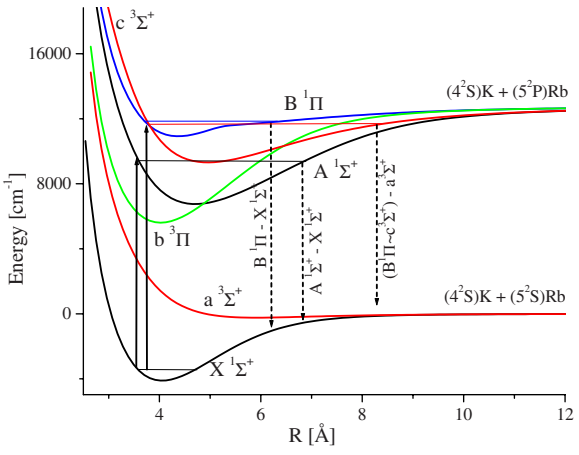

FIG. 1. (Color online) Theoretical potential energy curves for selected KRb states calculated in Ref. [11]. The schemes for laser excitation and the subsequent fluorescence are shown with solid and dashed arrows.

observed due to mixing with the nearby lying triplet states. Therefore in order to study the $a\,^3\Sigma^+$ state it was expected to follow straightforwardly the strategy which was successfully applied for the investigation of the same states in NaRb [1] and NaCs [2], i.e., to use the perturbations in the $B(1)^1\Pi$ state as a window to the triplet manifold.

II. EXPERIMENT

The KRb molecules were produced in a stainless steel heat pipe similar to that developed for NaRb [1] and NaCs [2]. Metallic K and Rb were mixed in an approximate mass ratio 1:1. The heat pipe was operated typically at a temperature of 550 K with 2–5 mbar of Ar as buffer gas. The laser-induced fluorescence (LIF) was excited with narrow band single mode lasers and resolved with a Fourier transform spectrometer (FTS) Bruker 120 HR.

For excitation of the $B(1)^1\Pi$ state we used a Coherent 599 linear laser with DCM dye delivering a power of about 70 mW. In the region between 15 000 cm^{-1} and 15 300 cm^{-1} we found a lot of transitions in the *B*-*X* band system. Along with them, transitions in the similar system of K_2 were often seen with comparable intensity. Going to higher frequencies the transitions in K_2 dominated those in KRb. It is worth noting here, that when we tested a heat pipe filled only with potassium, the fluorescence due to K_2 at similar experimental conditions (temperature, laser frequency, laser power) was at least a factor of 3 stronger than in the KRb heat pipe. Obviously in the case of mixtures the concentration of molecules cannot be derived simply from the saturated vapor pressure of the correspondent pure metals as often stated in spectroscopic papers. This is confirmed also by the fact that Rb_2 fluorescence was not observed in the studied spectral region, although Rb_2 was reported to absorb there [19–21].

The fluorescence from the *B* state led usually back to the ground $X\,^1\Sigma^+$ state. However, when exciting a perturbed level with triplet admixture, fluorescence down to the triplet state $a\,^3\Sigma^+$ was seen as well. It appeared in the region of 11 000–12 000 cm^{-1} well separated from the *B*-*X* fluorescence. An example is given in Fig. 2, where the fluorescence progression extends close to the dissociation asymptote, which can be concluded from the sharp decrease of the vibrational spacing below 10 950 cm^{-1}. When resolved by the FTS with a resolution of typically 0.03 cm^{-1} most lines to the $a\,^3\Sigma^+$ state show the expected hyperfine structure (HFS) similar to that observed in Refs. [1,2]. In those cases it could be explained by the Fermi contact interaction [22] using the atomic HFS parameters of Rb and K [23]. However, contrary to the NaRb andNaCs cases [1,2], there was also a large number of progressions, all lines of which show unusual HFS (see Fig. 3). This we shall discuss in Sec. III.

The ground state $X\,^1\Sigma^+$ was studied in Ref. [15] up to $v''=87$. The classical outer turning point of the last observed level is about 11.3 Å. This value differs from that given in the title of Ref. [15], namely, 10 Å, since the latter corresponds to the turning point of the level ($v''=87$, $J''=0$), but in fact the authors observed the vibrational level $v''=87$ for $J''=51$, which shifts the classical turning point to a larger internuclear distance. This distance, however is still too small in order to study the coupling between the $a\,^3\Sigma^+$ and $X\,^1\Sigma^+$ states due to the HFS mixing. Therefore, we revisited the $X\,^1\Sigma^+$ state asymptote in order to extend the experimental information closer to the dissociation limit. For this purpose we excited the $A\,^1\Sigma^+$-$X\,^1\Sigma^+$ system using a Ti:sapphire laser (from Tekhnoscan) pumped by a 10 W cw frequency doubled Nd:YAG laser (Coherent Verdi 10) and repeated as first steps measurements from Ref. [15] for internal calibration check. Then we extended the experimental data set by recording progressions from the same upper vibrational level but with different J'. It is worth noting that some of the lines of the progression reported in Ref. [15], which go to $v''=87$, turned out to be overlapped with stronger lines from different progressions. Exciting other upper vibrational levels that would give fluorescence to high lying ground state levels was not applicable due to the presence of strong K_2 fluorescence in the same spectral region.

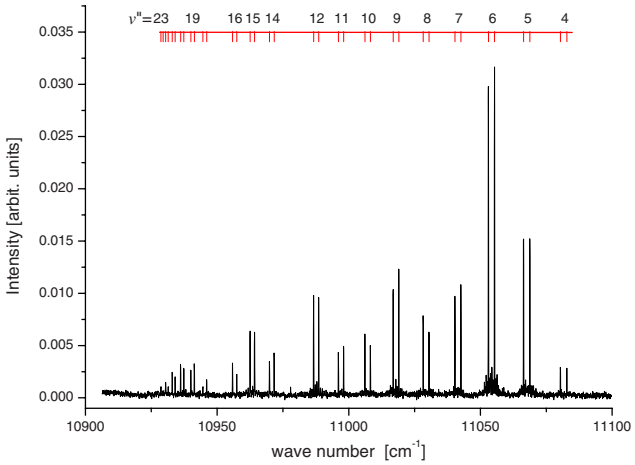

FIG. 2. (Color online) A fragment of a triplet progression excited at 15059.018 cm^{-1} and originating from (v',$J'=36$) in the *B*-*X* system. The doublets of the progression are formed by transitions to levels with $N''=36$ and 38 of the $a\,^3\Sigma^+$ state. For strong lines (e.g., $v''=6$) collisional satellites are also visible.

We searched also for transitions to the $a\,^3\Sigma^+$ state due to the so-called long-range changeover, which provided precious information in the case of NaRb [1] and LiCs [3]. By exciting a *B* state level close to the atomic asymptote [in those cases $(n^2S)+(m^2P)$] we actually approach the range where Hund's case (c) starts to be more appropriate than Hund's case (a) (due to the large fine structure splitting of the lowest *p* state in Rb and Cs). As a consequence, a decay from such excited levels to both $X\,^1\Sigma^+$ ($\Omega=0^+$) and $a\,^3\Sigma^+$ ($\Omega=1$ component) states is possible, which cannot be explained within the Hund's case (a) or (b) models either due to selection rules or due to vanishing Franck-Condon factors for the case of local perturbations. The case of KRb, however, turned out to be more similar to that of NaCs [2], where the long-range changeover appeared rather fragmentary and provided only few transitions to near asymptotic levels in the $X\,^1\Sigma^+$ and $a\,^3\Sigma^+$ states.

III. ANALYSIS

Our previous experience [1–3] has shown that the states $a\,^3\Sigma^+$ in the heteronuclear alkali-metal dimers can be mod-

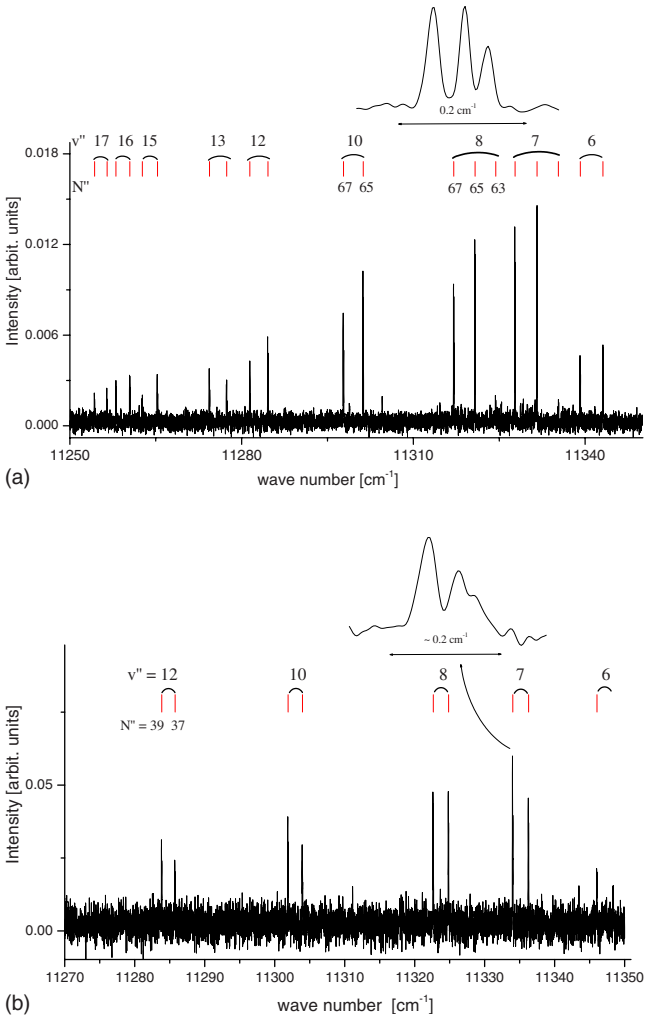

FIG. 3. (Color online) Examples of "usual" and "unusual" HFS within the progressions to the $a\ ^3\Sigma^+$ state. On the left side the progression starts from an upper state level with $J'=65$. The doublets are formed by transitions to levels with $N''=67$ and 65, except those with $v''=7$ and 8, where a weak transition to $N'=63$ also appears. On the right side a transition from $(v',J'=39)$ is shown. Both insets give examples of hyperfine structure (for details see text).

eled within the experimental resolution in the Born-Oppenheimer approximation by a single potential curve while the hyperfine splitting is well described within our resolution with the atomic hyperfine parameters. This is possible if the hyperfine structure does not depend on the internuclear separation. Only close to the atomic asymptote is it necessary to take into account the mixing with the ground state $X\ ^1\Sigma^+$.

The usual appearance of the hyperfine splitting of the $a\ ^3\Sigma^+$ levels is shown in the inset of Fig. 3(a) (the inset of the left graph). The splitting into three components is due to the interaction of the electrons with the nuclear spin of the Rb atom. Each of these components is further split due to the interaction with the K nuclear spin. This interaction is small, contrary to the case of Na in NaRb, for example [1], and is below our experimental resolution.

In the case of KRb we observed for the first time several progressions where the HFS differs from the expected one

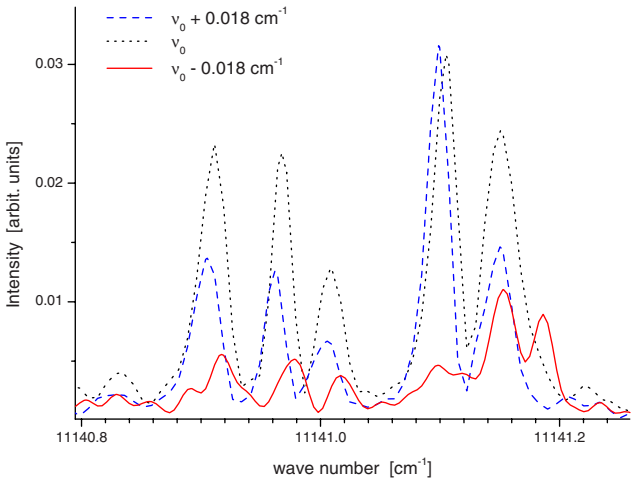

FIG. 4. (Color online) Two hyperfine groups of closely spaced transitions to $a\ ^3\Sigma^+$ state levels are shown for three different frequencies of the exciting laser. These transitions belong to different progressions, i.e., they originate from different excited levels $(v',J'=9$ and $v',J'=12)$. It is clearly seen that while the structure of the left transition [to the $(v''=6,N''=9)$ $a\ ^3\Sigma^+$ state level] remains almost unchanged and only the intensity varies, the overall pattern of the right transition [to the $(v''=6,N''=11)$ level] changes; for the blue and red detuned excitation frequencies, different components of the hyperfine triplet are missing.

[see the inset of Fig. 3(b)]. We made special efforts to study these "unusual" features within the possibilities of our experimental setup. We found out that within a given progression the hyperfine splitting is always independent of the rotational and vibrational quantum numbers of the $a\ ^3\Sigma^+$ state (both for the usual and the unusual cases). At the same time transitions to one given $a\ ^3\Sigma^+$ level coming from different excited levels can show different structure. Therefore, we concluded that it should be the structure of the upper state levels, which is responsible for the deviations from the expected HFS. This idea was confirmed by the observation that the unusual HFS changes its appearance when the excitation laser is detuned within the Doppler profile of the molecular transition. In Fig. 4 we show results of such an experiment. The laser simultaneously excites two transitions, one $[(v''=0,J''=9)\rightarrow(v',J'=9)]$ gives rise to a progression with usual HFS ($N''=7,9,11$ are involved [24]) and the second $[(v''=0,J''=11)\rightarrow(v',J'=12)$, the assignment of J' is not certain, which is unimportant for the analysis of the ground states]—with an unusual one ($N''=11,13$ are involved). We chose a portion of the fluorescence spectrum where two lines, each belonging to one of the progressions, appear closely together. Then we set the laser frequency within the Doppler profile of the transitions at three positions (center and $\pm 0.018\ \mathrm{cm}^{-1}$) and observed the change of the HFS of these lines. It is clearly seen in Fig. 4 that while the structure of the line with $N''=9$ remains almost unchanged and varies only in intensity, the overall pattern of the line with $N''=11$ changes. For the blue and red detuned excitation frequencies, different components of the hyperfine triplet are missing. Moreover, from the relative changes of the intensities of the lines from one laser frequency to another we can expect that

the effective widths of the excitation transitions are different. The transition producing the progression with unusual HFS could be broader, which is probably due to the HFS of the upper state level, being comparable with the Doppler width of the transition. This hypothesis seems to be reasonable if we compare it with the HFS of the $(2)^3\Sigma^+$ state in NaRb observed by Matsubara *et al.* in Ref. [25]. So, presently, we understand our observations in the following way: the HFS of the excited complex of singlet and triplet states in KRb is in some cases larger than the Doppler width of the transitions. The laser with given frequency excites a selected set of hyperfine components, which in turn does not give fluorescence to the full multiplet of the $a\ ^3\Sigma^+$ levels. Therefore, the observed structure of the spectral lines reflects the HFS both of the lower and the upper electronic states.

As a center frequency for a given hyperfine multiplet we chose the frequency of the central component of the HFS triplet (see the left part of Fig. 3), which is normally also the strongest. For the potential fit we used these frequencies and included the term energy of the upper level as a free parameter, common for all frequencies forming one progression. This selection is possible, because in a given progression the appearance of the HFS turned out to be independent of the vibrational and rotational quantum numbers within the experimental resolution. In case of progression with unusual HFS, we took a characteristic feature of the hyperfine group of lines (usually the strongest peak). In this way we were able to reproduce correctly the vibrational and rotational spacings of the $a\ ^3\Sigma^+$ state within a progression. We did not make efforts to reproduce the unusual HFS of the transitions, because our present understanding of the problem indicates that we need to also include the HFS of the upper state, the study of which is outside the scope of this work and would ask for a different experimental setup to get sufficient data for a convincing analysis.

A. $a\ ^1\Sigma^+$ state

Establishing the rotational numbering of the triplet progressions was straightforward because almost always they were accompanied by the corresponding progression to the ground $X\ ^1\Sigma^+$ state. For finding the proper vibrational numbering we first decided to rely on the possibility of scaling the molecular constants of one electronic state with the ratio of the reduced masses of different isotopomers. Experimentally, progressions belonging to the molecule with the less abundant isotope ^{87}Rb were easy to distinguish by the broader HFS compared to ^{85}Rb. In our initial analysis we had several progressions in ^{39}K^{85}Rb and one in ^{39}K^{87}Rb. The range of N'' [24] was from 31 to 68 and v'' spanning a range of 15 vibrational quanta. Several fits of Dunham-type coefficients with different vibrational assignment including both isotopomers indicated the most probable one which we took for further analysis of the experimental data and potential energy curve (PEC) construction.

Once the initial vibrational numbering was suggested, we fitted a potential curve for the $a\ ^3\Sigma^+$ state using a pointwise representation [26] and used it to assign new vibrational progressions. Periodically, as the size of the experimental data set significantly increased, the PEC was refined. We noticed, however, that for larger N'' there was a growing systematic disagreement between the observed and the calculated transition frequencies, which reached about 0.05 cm^{-1} for the highest N''. After all experimental data were assigned, this problem remained. Similarly to the $a\ ^3\Sigma^+$ state in NaRb [1], we can exclude the possibility for significant spin-rotational and second order spin-orbit effects in the $a\ ^3\Sigma^+$ state of KRb. Therefore, we searched for a connection between these systematic disagreements and the presence of unusual HFS of the transitions to the $a\ ^3\Sigma^+$ state levels—a phenomenon observed only in KRb up to now. Careful examination of the spectra and collection of new experimental observations proved that such a connection is not indicated by our data set. Therefore, we were forced to revise the initially established vibrational numbering, since our experience from the $a\ ^3\Sigma^+$ state in NaRb had shown that a wrong vibrational numbering could lead to similar systematic disagreements for high rotational quantum numbers. We tried several hypotheses of shifting v'' by up to two vibrational quanta and finally for one of them we got an excellent description of the whole data set within the experimental uncertainty. Now, for example, the levels with initial numbering $v=0$ suggested by the Dunham coefficients become $v=1$.

Here we want to direct special attention to this problem, because it is common practice to establish vibrational numbering by using the mass relations between the isotopes. Our experience in NaRb and KRb $a\ ^3\Sigma^+$ states demonstrates now, that given a limited set of levels with assigned rotational and vibrational quantum numbers, it is still possible to achieve an almost satisfactory quality of the fit assuming an incorrect vibrational assignment. In both molecules, discussed as examples here, we were able to construct PECs that fit the experimental data up to $N''=70$, but turned out to be systematically inadequate when going to higher N''. It is important to note also that in both cases the lowest vibrational levels ($v''=0-2$ for KRb) were not observed experimentally thus missing in the data field.

Finally, the analysis of our experimental data led to the assignment of 2400 transition frequencies to about 1100 rovibrational levels in the $a\ ^3\Sigma^+$ state in KRb. In Fig. 5 the range of the observed triplet state energy levels is presented. The full list of the transition frequencies is given in Table I of the supplementary material [32].

B. The $X\ ^1\Sigma^+$ state

After the assignment of the levels of the $a\ ^3\Sigma^+$ state and the derivation of a preliminary potential for it, we made first coupled channel calculations including the two states correlated to the $4s+5s$ atomic asymptote and the hyperfine interaction [1]. The purpose was to determine the region where the $X\ ^1\Sigma^+$ and $a\ ^3\Sigma^+$ states could be treated as uncoupled, and to use this region for fitting the PEC for the $a\ ^3\Sigma^+$ state. For the $X\ ^1\Sigma^+$ we took the potential given in Ref. [15], and extended it by the dispersion coefficients from Refs. [9,10]. These calculations indicated that the mixing between the two states is expected to be strong around $v''_X=86$ and exactly there we found the largest disagreement between the results

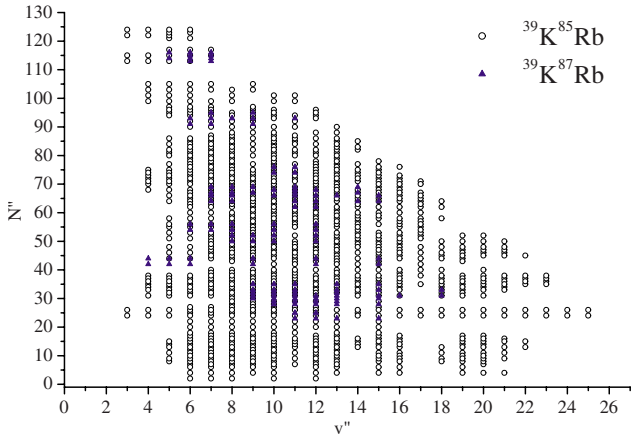

FIG. 5. (Color online) The range of vibrational and rotational quantum numbers of the energy levels of the $a\ ^3\Sigma^+$ state, observed in the present study.

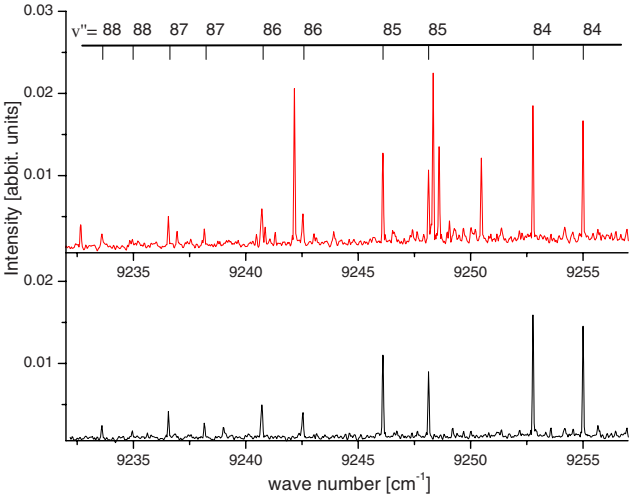

FIG. 6. (Color online) A portion of progressions from the same upper state level (v',$J'=51$), but excited from different lower $X\ ^1\Sigma^+$ state levels: ($v''=9$, $J''=50$) for the upper trace and ($v''=8$, $J''=52$) for the lower trace.

of the single channel fit and the experimental observation. This disagreement, however, could not be fully explained even after the coupling was taken into account. Therefore, we decided to reinvestigate experimentally the highest levels of the ground state in KRb, trying to collect higher vibrational levels with a wider range of J''.

Due to better signal-to-noise ratio in our experiment we were able to extend the highest observed vibrational quantum number to $v''=88$. The corresponding levels were observed for $J''=51-55$. The assignment of the observed transitions was based on the analysis of Ref. [15]. As already mentioned in Sec. II the weak KRb progressions close to the asymptote were overlapped by stronger K_2 transitions. Apparently, this led to an incorrect determination of the transition frequency to the ($v''=86$, $J''=52$) level in Ref. [15] by about 0.02 cm^{-1}. In order to increase the confidence in our assignment and avoid similar situations we excited the same upper level from different $X\ ^1\Sigma^+$ levels. Thus, KRb lines of interest should be the same, but overlapping KRb or K_2 lines should be shifted or disappear. As an example, we show in Fig. 6 progressions starting from (v',$J'=51$), excited from ($v''=9$, $J''=50$) for the upper trace, and ($v''=8$, $J''=52$) for the lower trace. The same progression is shown also in Fig. 1 of Ref. [15], but there excited from ($v''=9$, $J''=52$). By a simple inspection it is immediately clear what lines appear in both traces and are thus the desired KRb lines. Overall, the present experiment brings 1200 additional lines to the data set of the $X\ ^1\Sigma^+$ state.

In order to make a reliable connection in the energy scale between the $X\ ^1\Sigma^+$ and the $a\ ^3\Sigma^+$ states we added to the ground state data set also levels of progressions (about 600 transitions) that were recorded simultaneously with progressions to the triplet state and originating both from a common upper state level. In this way we add in total about 1800 new transition frequencies to the primary data set obtained in Ref. [15].

IV. POTENTIALS

The full description of the experimental data needs a model including adiabatic PECs of the two electronic states and parameters that describe the coupling between them due to the hyperfine interaction. Similarly to the approach adopted in Refs. [1,2] we first constructed the potentials using single channel fits and then we performed coupled channels calculations and determined the shifts due to the interaction between the states. As a next step, we corrected the experimental data with the calculated corrections, obtaining in this way "adiabatic" data sets, i.e., data sets that would have been observed if the states would not couple. Afterwards the whole procedure was repeated until the results of the coupled channels calculations agreed with the experimental observations.

For the potential construction we first used the pointwise representation. In the initial stages of fitting it has the advantage to be very flexible, achieving a convergence in only a few iterations. In this way the potential curve was refined following the growth of the experimental data set, several hypotheses of the vibrational numbering in the $a\ ^3\Sigma^+$ state were tested, and also some wrong line assignments were identified. For the coupled channels fit the pointwise potentials were transformed into analytic form [27] with which the number of free parameters is reduced by almost a factor of two.

We split the representation of the potentials into three regions: the repulsive wall ($R<R_{\mathrm{inn}}$), the asymptotic region ($R>R_{\mathrm{out}}$), and the intermediate region in between. The analytic form of each potential in the intermediate range is described by a finite power expansion with a nonlinear variable function ξ of internuclear separation R as follows:

$$\xi(R)=\frac{R-R_m}{R+bR_m}, \tag{1}$$

$$U_{\mathrm{IR}}(R)=\sum_{i=0}^{n} a_i \xi(R)^i, \tag{2}$$

where $\{a_i\}$ are fitting parameters and b and R_m are chosen during the transform process from the spline representation

TABLE I. Parameters of the analytic representation of the $X\,^1\Sigma^+$ state potential. The energy reference is the dissociation asymptote. Parameters with * are set for continuous extrapolation of the potential.

$R < R_{\text{inn}} = 3.000$ Å	
A^*	-0.731001924×10^4 cm^{-1}
B^*	0.590300435×10^6 cm^{-1} Å^4
$R_{\text{inn}} \le R \le R_{\text{out}} = 11.000$ Å	
b	−0.39
R_m	4.06818602 Å
a_0	−4217.814754 cm^{-1}
a_1	$0.5530165860346669 \times 10^1$ cm^{-1}
a_2	$0.1402690940409950 \times 10^5$ cm^{-1}
a_3	$0.1048318435177453 \times 10^5$ cm^{-1}
a_4	$-0.4087971898030580 \times 10^4$ cm^{-1}
a_5	$-0.1817659880541463 \times 10^5$ cm^{-1}
a_6	$-0.2739889053154796 \times 10^5$ cm^{-1}
a_7	$-0.3930730951201573 \times 10^5$ cm^{-1}
a_8	$0.1755013192862486 \times 10^6$ cm^{-1}
a_9	$0.4366867152340260 \times 10^6$ cm^{-1}
a_{10}	$-0.6031147948206772 \times 10^7$ cm^{-1}
a_{11}	$-0.7948028201366105 \times 10^7$ cm^{-1}
a_{12}	$0.1172293247025888 \times 10^9$ cm^{-1}
a_{13}	$0.9209455256556711 \times 10^8$ cm^{-1}
a_{14}	$-0.1533597323741656 \times 10^{10}$ cm^{-1}
a_{15}	$-0.6982526182585652 \times 10^9$ cm^{-1}
a_{16}	$0.1418207140035536 \times 10^{11}$ cm^{-1}
a_{17}	$0.3514113318792982 \times 10^{10}$ cm^{-1}
a_{18}	$-0.9529625435553510 \times 10^{11}$ cm^{-1}
a_{19}	$-0.1096758619400216 \times 10^{11}$ cm^{-1}
a_{20}	$0.4743826569413903 \times 10^{12}$ cm^{-1}
a_{21}	$0.1477139521952726 \times 10^{11}$ cm^{-1}
a_{22}	$-0.1768149926253122 \times 10^{13}$ cm^{-1}
a_{23}	$0.3496665669778944 \times 10^{11}$ cm^{-1}
a_{24}	$0.4947896972615874 \times 10^{13}$ cm^{-1}
a_{25}	$-0.2373506540656795 \times 10^{12}$ cm^{-1}
a_{26}	$-0.1033913349509970 \times 10^{14}$ cm^{-1}
a_{27}	$0.6234843170080333 \times 10^{12}$ cm^{-1}
a_{28}	$0.1588626857834081 \times 10^{14}$ cm^{-1}
a_{29}	$-0.9740574795906707 \times 10^{12}$ cm^{-1}
a_{30}	$-0.1741861156434701 \times 10^{14}$ cm^{-1}
a_{31}	$0.9410306699092036 \times 10^{12}$ cm^{-1}
a_{32}	$0.1289614354386887 \times 10^{14}$ cm^{-1}
a_{33}	$-0.5220986485346664 \times 10^{12}$ cm^{-1}
a_{34}	$-0.5776754651606419 \times 10^{13}$ cm^{-1}
a_{35}	$0.1278431437418345 \times 10^{12}$ cm^{-1}
a_{36}	$0.1182411100178171 \times 10^{13}$ cm^{-1}
$R_{\text{out}} < R$	
U_∞	0.0 cm^{-1}
C_6	0.2072097×10^8 cm^{-1} Å^6
C_8	0.6509487×10^9 cm^{-1} Å^8
C_{10}	0.2575245×10^{11} cm^{-1} Å^{10}
A_{ex}	0.1469387×10^5 cm^{-1} Å$^{-\gamma}$
γ	5.25669
β	2.11445 Å^{-1}
Derived constants:	
Equilibrium distance:	$R_e^X = 4.06770(5)$ Å
Electronic term energy:	$T_e^X = -4217.815(10)$ cm^{-1}

to the analytic one; R_m is close to the value of the equilibrium separation. The potential is continuously extrapolated for $R < R_{\text{inn}}$ with

$$U_{\text{SR}}(R) = A + B/R^4 \tag{3}$$

by adjusting the A and B parameters.

For large internuclear distances ($R > R_{\text{out}}$) we adopted the standard long-range form of molecular potentials as follows:

$$U_{\text{LR}}(R) = U_\infty - C_6/R^6 - C_8/R^8 - C_{10}/R^{10} \pm E_{\text{exch}}, \tag{4}$$

where the exchange contribution is given by

$$E_{\text{exch}} = A_{\text{ex}} R^\gamma \exp(-\beta R), \tag{5}$$

and U_∞ is the energy of the atomic asymptote (excluding the hyperfine energies) with respect to the minimum of the $X\,^1\Sigma^+$ state. It coincides with the dissociation energy of this state, D_e^X. The exchange energy is repulsive for the triplet state [plus sign in Eq. (4)] and attractive for the singlet state (minus sign). All parameters in Eqs. (4) and (5) are common for the $X\,^1\Sigma^+$ and the $a\,^3\Sigma^+$ states.

As a first guess we used the theoretical estimates of long-range parameters published by Dervianko *et al.* and Porsev *et al.* [9,10] for the $X\,^1\Sigma^+$ and the triplet $a\,^3\Sigma^+$ state. For the exchange energy amplitude we adopted the estimation from theoretical potentials in Ref. [11]. The continuation at R_{out} was obtained smoothly by variation of U_∞ or a_0, the latter is preferred because the dissociation asymptote is taken as common energy reference for both states and set to zero here.

For the coupled channels calculations the hyperfine interaction is taken into account as caused by the Fermi contact interaction. The effective Hamiltonian for the electronic spin **S** and the nuclear spin **I** defines the interaction parameters as follows:

$$H = A_{\text{Rb}} S_{\text{Rb}} I_{\text{Rb}} + A_{\text{K}} S_{\text{K}} I_{\text{K}}. \tag{6}$$

From the experimental spectra the A_{K} and A_{Rb} constants could be determined applying Hund's case $b_{\beta S}$ as the basis. Generally, the molecular coupling parameters correspond to the atomic constants A. But for atoms forming a diatomic molecule the dependence of these parameters on the bond length and thus on the vibrational and rotational quantum numbers cannot be excluded (see Ref. [28]). Within the resolution of our experiment we recorded partially resolved hyperfine structure of the levels of the $a\,^3\Sigma^+$ state and since our data covered a broad range of such levels we checked the dependence of A_{K}, A_{Rb}^{85}, and A_{Rb}^{87} on vibrational and rotational quantum numbers. As obtained in other cases of mixed alkali-metal dimers the observed hyperfine splitting is described within experimental accuracy by using the atomic parameters as compiled by Arimondo [23]. Then, each special case of strong coupling between the singlet and the triplet levels is well described by the coupled channels calculations.

With the definitions by Eqs. (1)–(6), the iteration process of potential fitting and the calculation of the corrections by singlet-triplet coupling was performed on all spectroscopic observations of the $X\,^1\Sigma^+$ state from Ref. [15] and from the present work and of the $a\,^3\Sigma^+$ state. It is especially important

to note that we obtained a large set of fluorescence progressions to $X\ ^1\Sigma^+$ and $a\ ^3\Sigma^+$ with a common excited level, which fixes the relative energy position of singlet and triplet level schemes precisely and gives information on the exchange energy from levels close to the dissociation asymptote. In total, 12 502 transition frequencies were contained in the fit and 68 free parameters were varied, which gave a dimensionless standard deviation $\sigma=0.68$ for both states together. Tables I and II present these parameters, but the values actually given there are from the final step of fitting described in the following section including data from cold collision studies of other authors. For the convenience of the reader also the position of the potential minimum in energy (T_e) and internuclear separation (R_e) are given in both tables.

V. COLD COLLISIONS

As it was already mentioned in the Introduction, Feshbach resonances for $^{40}K^{87}Rb$ were observed by several groups [5,6]. In this section we apply the derived potentials to calculate these Feshbach resonances and compare them with observations. It is important to note that the spectroscopic observations of the present study were done on different isotopomers, thus application of the derived potentials for the Feshbach resonances assumes the validity of the Born-Oppenheimer approximation within the desired accuracy. We use for the comparison the *s*-wave resonances observed in Ref. [5], because these data represent the largest set and come from the same lab, thus they should not show possible internal inconsistency like calibration errors of the magnetic field. All calculated resonances were found within 50 Gauss from the observed ones; this deviation is not surprisingly large because these calculations are extrapolations out of the range of spectroscopic observations; the largest outer turning point of observed levels is at 12.6 Å for the singlet state and at 14.8 Å for the triplet state being 6.4 and 2.3 cm^{-1} below the dissociation asymptote, respectively. This indicates that the spectroscopic observation ends within the changeover to the long-range behavior and the quality of the extrapolation follows more from the reliability of the theoretical estimates of the dispersion coefficients [9,10] than from our experimental data.

Thus the measured Feshbach resonances contain information on the long-range function. To include them in the total potential determination we set up a nonlinear least squares fitting code for the dispersion parameters, which contains the scattering calculations as subroutine and searches for the maximum of the elastic rate coefficient, which corresponds to the observed Feshbach resonance. The resonances have been observed by trap loss of potassium, thus by an inelastic process, which will need three body collisions. As very often assumed, the three body cross section should be enhanced by the condition of a two body Feshbach resonance. The calculations were done for a temperature of 1 μK and use the accuracy of the magnetic field of 0.2 G, as stated in Ref. [4], as uncertainty for each individual observation. In a first step the resonances were fitted by varying the dispersion terms C_6 and C_8, only. With the new total potentials asymptotic levels of pure singlet ($v=97,98,99$) and triplet ($v=29,30,31$) states

TABLE II. Parameters of the analytic representation of the $a\ ^3\Sigma^+$ state potential. The energy reference is the dissociation asymptote. Parameters with * are set for continuous extrapolation of the potential.

$R<R_{inn}=4.956$ Å	
A^*	-0.102755858×10^4 cm^{-1}
B^*	0.595720017×10^6 cm^{-1} Å^4
$R_{inn}\le R\le R_{out}=11.000$ Å	
b	−0.41
R_m	5.90210000 Å
a_0	−249.030467 cm^{-1}
a_1	−0.8249570532852936 cm^{-1}
a_2	$0.1696361682907917\times10^4$ cm^{-1}
a_3	$0.2195618553936388\times10^4$ cm^{-1}
a_4	$-0.1830331320330776\times10^5$ cm^{-1}
a_5	$-0.3577610246567447\times10^6$ cm^{-1}
a_6	$0.7605943179592050\times10^6$ cm^{-1}
a_7	$0.2321948211354688\times10^8$ cm^{-1}
a_8	$-0.2969108359066523\times10^8$ cm^{-1}
a_9	$-0.9066958465430735\times10^9$ cm^{-1}
a_{10}	$0.1193993210361681\times10^{10}$ cm^{-1}
a_{11}	$0.2271299134652605\times10^{11}$ cm^{-1}
a_{12}	$-0.3822195877987927\times10^{11}$ cm^{-1}
a_{13}	$-0.3733663448209457\times10^{12}$ cm^{-1}
a_{14}	$0.8258881465522462\times10^{12}$ cm^{-1}
a_{15}	$0.3983625994810529\times10^{13}$ cm^{-1}
a_{16}	$-0.1170134952322679\times10^{14}$ cm^{-1}
a_{17}	$-0.2572921814049761\times10^{14}$ cm^{-1}
a_{18}	$0.1083172601973219\times10^{15}$ cm^{-1}
a_{19}	$0.7316944602806914\times10^{14}$ cm^{-1}
a_{20}	$-0.6401304321393455\times10^{15}$ cm^{-1}
a_{21}	$0.2090674461383090\times10^{15}$ cm^{-1}
a_{22}	$0.2236346785424132\times10^{16}$ cm^{-1}
a_{23}	$-0.2555345293959939\times10^{16}$ cm^{-1}
a_{24}	$-0.3556041967731776\times10^{16}$ cm^{-1}
a_{25}	$0.8321268009266810\times10^{16}$ cm^{-1}
a_{26}	$-0.1364612053210692\times10^{16}$ cm^{-1}
a_{27}	$-0.9030566262973000\times10^{16}$ cm^{-1}
a_{28}	$0.8950177388640356\times10^{16}$ cm^{-1}
a_{29}	$-0.2723988913077922\times10^{16}$ cm^{-1}
$R_{out}<R$	
U_∞	0.0 cm^{-1}
C_6	0.2072097×10^8 cm^{-1} Å^6
C_8	0.6509487×10^9 cm^{-1} Å^8
C_{10}	0.2575245×10^{11} cm^{-1} Å^{10}
A_{ex}	-0.1469387×10^5 cm^{-1} Å$^{-\gamma}$
γ	5.25669
β	2.11445 Å^{-1}
Derived constants:	
Equilibrium distance:	$R_e^a=5.9029(1)$ Å
Electronic term energy:	$T_e^a=-249.031(10)$ cm^{-1}

TABLE III. Comparison of scattering lengths [in Bohr radius ($a_0=0.5292\times10^{-10}$ m)].

	a_{singlet}		a_{triplet}		a_{lowest}	
Isotope	Ref. [5]	Present	Ref. [5]	Present	Ref. [5]	Present
39/85	26.5(9)	33.4	63.0(5)	63.9	56.6(4)	58.0
39/87	824^{+90}_{-70}	1868	35.9(7)	35.90	27.9(9)	28.36
40/85	64.5(6)	65.8	−28.4(16)	−28.55	−25.3(16)	−21.12
40/87	−111(5)	−111.5	−215(10)	−215.6	−185(7)	−183.1
41/85	106.0(8)	103.1	348(10)	349.8	283(6)	283.6
41/87	14.0(11)	7.06	163.7(16)	164.4	1667^{+790}_{-406}	647.8

were calculated and used as input for a new fit of the single channel calculations. Error limits for these levels were estimated from the fit of the resonances to be about 100 kHz. In the new fit of the inner part of the potentials the coefficient C_{10} was chosen as an additional free parameter. With this result a new iteration was started. Only two such iterations, resonance fit followed by single channel fit, were needed for convergence. The final results are given in Table I for the $X\,^1\Sigma^+$ state and in Table II for the $a\,^3\Sigma^+$ state.

The ten *s*-wave Feshbach resonances could be fitted to a standard deviation of $\sigma=1.37$ and show on average a systematic deviation of +0.05 G, i.e., the observations are at larger magnetic fields than the results from the fit. This fit of the resonances is slightly better than the one published in Ref. [5]: $\sigma=1.66$ and mean deviation +0.04 G, and has the additional advantage, that all spectroscopic observations are equally well described as stated in the previous section. All long-range parameters are close to the theoretical predictions [9,10], which indicates that we have obtained a physically consistent model for the two electronic states correlated to the atomic ground states $(4s)$K+$(5s)$Rb. It will be applied now to calculate an overview of expected collision properties at low kinetic energy, the upper limit of which is not easy to estimate because of the artificial repulsive branches of the potentials [see Eq. (3)].

Ferlaino *et al.* [5] give a list of singlet and triplet scattering lengths for all possible isotope combinations of KRb with natural abundance and calculate the scattering length of the lowest hyperfine input channel of KRb. For the application of mass scaling they used full potentials from other sources which give for ^{40}K^{87}Rb as the number of supported vibrational levels 98 for singlet and 32 for triplet. The potentials derived in the present work support also 32 for triplet, however, 100 for singlet. Such possible variation was taken into account by the error limits stated in Ref. [4]. Table III compares our results with those from Ferlaino *et al.* The two columns, labeled as a_{lowest}, show scattering lengths of the lowest Zeeman level in each case of the isotope pair, e.g., for ^{39}K+^{85}Rb $f_{\text{K}}=1$, $m_{\text{K}}=1$ and $f_{\text{Rb}}=2$, $m_{\text{Rb}}=2$.

Certainly, for ^{40}K^{87}Rb the results closely agree, but for the other isotopomers significant differences, especially for the singlet case appear, which reflects the different number of supported vibrational levels within the respected potentials of this state.

In the experiments by Ferlaino *et al.* [5] and Ospelkaus *et al.* [6] also *p*-wave resonances and *s*-wave resonances coupled to *d* levels are reported. We checked if these are also well described with the present potentials. Especially in Ref. [6] the splitting between $m_l=0$ and $m_l=\pm1$ of a *p* wave is reported and it gives the opportunity to check if the spin-spin or second order spin-orbit coupling for the triplet state needs to be adjusted which both together can be described by the effective operator [29] as follows:

$$H_{\text{SS}}=\frac{2}{3}\lambda(3S_z^2-S^2). \tag{7}$$

λ is a function of the internuclear separation R and typically is derived from spectroscopic data as an expectation value of a specific vibrational level. Here we use simple functional forms to incorporate the pure dipole-dipole contribution for the spin-spin interaction as a function $1/R^3$ and the spin-orbit part as an exponential function reflecting effectively an overlap integral of the electronic distribution of the two atoms:

$$\lambda_{\text{SS}}=-\frac{3}{4}\alpha^2\left(\frac{1}{R^3}+a_{\text{SO}}\exp[-b(R-R_{\text{SO}})]\right). \tag{8}$$

All quantities are given in atomic units, α is the fine structure constant, and a_{SO}, b, and R_{SO} are the model parameters for the second order spin-orbit contribution. Since the data in hand cannot be sensitive to the actual function, we selected values for b and R_{SO}, which are comparable to the example of Rb_2 [30] ($b=0.7196a_0^{-1}$ and $R_{\text{SO}}=7.5a_0$) and fitted the parameter a_{SO}, which gives $a_{\text{SO}}=-0.013a_0^{-3}$ ($a_0=0.5292\times10^{-10}$ m). The result shows that the first part in Eq. (8) dominates in the internuclear separation interval $R>12a_0$ important for the bound levels of the triplet state, which determine the Feshbach resonances.

Taking this result into account, the four resonances reported in Refs. [5,6] involving $l=1$ and 2 were calculated. The $l=1$ resonances were found within the experimental accuracy, and it is predicted that the resonance at 456 G is split for $m_l=0,\pm1$ by about 0.1 G, where the component $m_l=0$ is higher in field than the others. This is opposite to the case of the observed resonance at 515 G. The $l=2$ resonances were found above the observed magnetic field but not more than 0.7 G; the reason for this difference is presently unclear. These resonances are very sharp; the calculated rate constants of the corresponding elastic collisions have half widths of less than 0.001 G, which depends on the magnitude of the above mentioned SS coupling. No value was given in [5] for their calculations of the widths.

VI. CONCLUSIONS

An extensive data set on the $a\,^3\Sigma^+$ state of KRb was collected covering energy levels in a wide range of vibrational and rotational quantum numbers in ^{39}K^{85}Rb and ^{39}K^{87}Rb. The classical turning point of the last observed level ($v''=25$, $J''=26$) lies at 14.6 Å on the fitted rotationless potential energy curve. The long-range parameters C_6, C_8, and C_{10} deviate only slightly from the theoretical estimates in Refs. [9,10], but we should remind the reader, that the present data set does not allow one to determine independently all three parameters. Thus due to correlations between those of the

data analysis, there is no contradiction to those of the theory. But for modeling of cold collisions one should use the values reported in Tables I and II of the present work.

The complete determination of the potential curves allows for reliable extrapolation to the dissociation limit and thus determination of their depths. Tables I and II give 4217.815(10) cm^{-1} and 249.031(10) cm^{-1} for the respective dissociation energies. Recently, Wang *et al.* [31] reported about an independent determination of the dissociation energy of the singlet state using a photoassociation-depletion process to obtain binding energies of loosely bound vibration levels, namely, $v''=87$ and 89. The dissociation energy was derived by adding level energies with respect to the minimum of the potential curve as reported in Ref. [15] by a near-dissociation expansion (NDE) approach. The final value 4217.822(3) cm^{-1} agrees with ours within the given error limits. But for estimating the error limit Wang *et al.* assume that the accuracy of level energy $v''=87$ is equal to the standard deviation of the NDE fit, 0.0015 cm^{-1}. Looking into the actual data set from Ref. [15] one finds that for $v''=87$ only two high rotational states with $J''=50$ and 52 were observed. Thus a fairly far extrapolation to the levels with $J''=0$ is done, and one should certainly include the correlation of the NDE parameters for the error estimation. Additionally, we would remind the reader that we corrected a misidentification of $v''=86$ levels, due to overlapping lines, and this would affect the NDE analysis. Therefore, the good agreement between our present dissociation energy and that reported by Wang *et al.* could be fortunate. As a second check we calculated the binding energies for $v''=87$ and 89 from our results and found them larger by 0.026 and 0.053 cm^{-1}, respectively. For $v''=87$ the deviation is about 12 times the error limit reported by Wang *et al.* We tried to incorporate the measured binding energies in a new fit of the potentials including our spectroscopic results and the Feshbach resonances from Ref. [5], but no convincing result was obtained up to now. The reason for the discrepancy is unclear for us, especially because we extended the data set from Ref. [15] just around $v''=87$ with more J levels and by measurements with $v''=88$. Thus the energy interval where the $v''=87$ is located is well covered by our measurements, which have an accuracy of typically 0.003 cm^{-1}.

By new spectroscopic data the potential curve of the $X\ ^1\Sigma^+$ state could be refined compared to the work by Ref. [15], and we were able to link it to the potential curve of the $a\ ^3\Sigma^+$ state with respect to the asymptotic function and to the relative energy position of both functions. This was the prerequisite to start the inclusion of the observed Feshbach resonances [4] into the modeling, which finally leads to a complete system for predicting ultracold collision properties. Such a prediction can be extended to other isotopomers, as presented partly in Table III. But it would be clearly desirable to get precise Feshbach resonances also for different isotopomers in order to check the degree of validity of the Born-Oppenheimer approximation.

Despite the combination of the spectroscopic and Feshbach data there is a significant gap in the energy interval below the atomic asymptote (about 3 cm^{-1}) in which bound levels of low rotational quantum numbers, preferably J or $N=0$, could be observed. Thus the prediction in this region relies on the quality of the long-range parameters and measurements, e.g., by two-color photoassociation would be valuable. To reach such levels by Feshbach spectroscopy is not promising because too high magnetic fields would be needed.

KRb is very often discussed for applications in studies of dipolar cold gases or even quantum computing. To transfer Feshbach molecules to deeply bound levels, which are stable and would have large electric dipole moments, spectroscopic data on excited states will be of importance to predict efficient processes. Such data are partly existing from other authors and are on hand also from our own spectroscopic work, which will be analyzed joining the available data. Of particular interest in KRb is the HFS in the $B^1\Pi$ state, which is supposed to cause the "irregular" hyperfine splitting of the transitions to the $a\ ^3\Sigma^+$ state.

ACKNOWLEDGMENTS

We gratefully acknowledge C. Amiot for providing us with his complete experimental data in electronic form. This work is supported by DFG through Grants No. SFB 407 and No. GRK 665. O.D., M.T., and R.F. acknowledge the support by the NATO Optical Field Mapping Grant No. SfP 978029 and by the Latvian Science Council Grant No. 04.1308. O.D. acknowledges the support from the European Social Fund and A.P.—partial support from the Bulgarian National Science Fund Grants No. MUF 1506/05 and No. VUF 202/06.

[1] A. Pashov, O. Docenko, M. Tamanis, R. Ferber, H. Knoeckel, and E. Tiemann, Phys. Rev. A **72**, 062505 (2005).
[2] O. Docenko, J. Zaharova, M. Tamanis, R. Ferber, A. Pashov, H. Knöckel, and E. Tiemann, J. Phys. B **39**, S929 (2006).
[3] P. Staanum, A. Pashov, H. Knöckel, and E. Tiemann, Phys. Rev. A **75**, 042513 (2007).
[4] F. Ferlaino, C. D'Errico, G. Roati, M. Zaccanti, M. Inguscio, G. Modugno, and A. Simoni, Phys. Rev. A **73**, 040702(R) (2006).
[5] F. Ferlaino, C. D'Errico, G. Roati, M. Zaccanti, M. Inguscio, G. Modugno, and A. Simoni, Phys. Rev. A **74**, 039903(E) (2006).
[6] S. Ospelkaus, C. Ospelkaus, L. Humbert, K. Sengstock, and K. Bongs, Phys. Rev. Lett. **97**, 120403 (2006).
[7] B. Bussery, Y. Achkar, and M. Aubert-Frecon, Chem. Phys. **116**, 319 (1987).
[8] M. Marinescu and H. R. Sadeghpour, Phys. Rev. A **59**, 390 (1999).
[9] A. Dervianko, J. F. Babb, and A. Dalgarno, Phys. Rev. A **63**, 052704 (2001).
[10] S. G. Porsev and A. Dervianko, J. Chem. Phys. **119**, 844 (2003).

[11] S. Rousseau, A. R. Allouche, and M. Aubert-Frécon, J. Mol. Spectrosc. **203**, 235 (2000).
[12] S. J. Park, Y. J. Choi, Y. S. Lee, and G.-H. Jeung, Chem. Phys. **257**, 135 (2000).
[13] S. Kotochigova, P. S. Julienne, and E. Tiesinga, Phys. Rev. A **68**, 022501 (2003); J. Mol. Spectrosc. **203**, 235 (2000).
[14] A. J. Ross, C. Effantin, P. Crozet, and E. Boursey, J. Phys. B **23**, L247 (1990).
[15] C. Amiot and J. Vergés, J. Chem. Phys. **112**, 7068 (2000).
[16] T. Leininger, H. Stoll, and G.-H. Jeung, J. Chem. Phys. **106**, 2541 (1997).
[17] S. Kasahara, Ch. Fujiwara, N. Okada, H. Kato, and M. Baba, J. Chem. Phys. **111**, 8857 (1999).
[18] C. Amiot, J. Vergés, J. d'Incan, and C. Effantin, Chem. Phys. Lett. **321**, 21 (2000).
[19] C. Amiot, J. Chem. Phys. **93**, 8591 (1993).
[20] C. Amiot and J. Vergés, Chem. Phys. Lett. **274**, 91 (1997).
[21] C. D. Caldwell, F. Engelke, and H. Hage, Chem. Phys. **54**, 21 (1980).
[22] S. Kasahara, T. Ebi, M. Tanimura, H. Ikoma, K. Matsubara, M. Baba, and H. Katô, J. Chem. Phys. **105**, 1341 (1996).
[23] E. Arimondo, M. Inguscio, and P. Violino, Rev. Mod. Phys. **49**, 31 (1977).
[24] The appropriate rotational quantum number for the $a\ ^3\Sigma^+$ state is N in the Hund's case (b).
[25] K. Matsubara, Y.-C. Wang, K. Ishikawa, M. Baba, A. J. McCaffery, and H. Katô, J. Chem. Phys. **99**, 5036 (1993).
[26] A. Pashov, W. Jastrzębski, and P. Kowalczyk, Comput. Phys. Commun. **128**, 622 (2000).
[27] C. Samuelis, E. Tiesinga, T. Laue, M. Elbs, H. Knöckel, and E. Tiemann, Phys. Rev. A **63**, 012710 (2000).
[28] H. Knöckel, B. Bodermann, and E. Tiemann, Eur. Phys. J. D **28**, 199 (2004).
[29] E. Hirota, J. M. Brown, J. T. Hougen, T. Shida, and N. Hirota, Pure Appl. Chem. **66**, 571 (1994).
[30] F. H. Mies, C. J. Williams, P. S. Julienne, and M. Kraus, J. Res. Natl. Inst. Stand. Technol. **101**, 521 (1996).
[31] D. Wang, J. T. Kim, C. Ashbaugh, E. E. Eyler, P. L. Gould, and W. C. Stwalley, Phys. Rev. A **75**, 032511 (2007).
[32] See EPAPS Document No. E-PLRAAN-76-160708 for a full list of transition frequencies. For more information on EPAPS, see http://www.aip.org/pubservs/epaps.html.